

~~RESTRICTED~~

Copy No.
RM No. L7K28

NACA RM No. L7K28

7 JUL 1948
CLASSIFICATION CANCELLED

NACA Release form 726, dated 2-28-52.
H. L. Dryden for NACA

NAR

4-9-52

RESEARCH MEMORANDUM

HIGH-SPEED WIND-TUNNEL INVESTIGATION OF A FLYING-BOAT
HULL WITH HIGH LENGTH-BEAM RATIO

By

John M. Riebe and Rodger L. Naeseth

Langley Memorial Aeronautical Laboratory
Langley Field, Va.

CLASSIFIED DOCUMENT

This document contains classified information affecting the National Defense of the United States within the meaning of the Espionage Act, USC 50131 and 50132. Its transmission or the revelation of its contents in any manner to an unauthorized person is prohibited by law. Information so classified may be imparted only to persons in the military and naval services of the United States, appropriate civilian officers and employees of the Federal Government who have a legitimate interest therein, and to United States citizens of known loyalty and discretion who of necessity must be informed thereof.

NATIONAL ADVISORY COMMITTEE
FOR AERONAUTICS

WASHINGTON
June 30, 1948

~~RESTRICTED~~

LANGLEY MEMORIAL AERONAUTICAL
LABORATORY
Langley Field, Va.

NATIONAL ADVISORY COMMITTEE FOR AERONAUTICS

RESEARCH MEMORANDUM

HIGH-SPEED WIND-TUNNEL INVESTIGATION OF A FLYING-BOAT

HULL WITH HIGH LENGTH-BEAM RATIO

By John M. Riebe and Rodger L. Naeseth

SUMMARY

An investigation was made in the Langley 7- by 10-foot high-speed tunnel to determine the effect of Mach number on the aerodynamic characteristics of a flying-boat hull with high length-beam ratio. For comparison, tests were made on a streamline body simulating the fuselage of a modern transport airplane.

The hull, made by extending the afterbody and fairing the nose of Langley tank model 214, had a minimum drag coefficient of 0.0060 at 0.4 Mach number including the interference of the thin sweptback support wing; the minimum drag coefficient of the streamline body was 0.0030. Increasing Mach number resulted in drag coefficient increases for both hull and fuselage at all angles of attack investigated; the rate of increase became smaller as the body was made more refined. At 0° angle of attack the drag coefficients were 0.0023, 0.0021, 0.0017, and 0.0008 larger at 0.8 Mach number than at 0.4 Mach number for the hull, hull with step fairing, hull with rounded bottom, and streamline body, respectively. Angles of attack for minimum drag in the positive range extended from 0° to about 4° for the hull and 0° to about 2° for the streamline body for all Mach numbers at which data were not limited to low angles of attack.

Increasing Mach number resulted in a very slight decrease in longitudinal stability for both hull and fuselage; directional stability was generally constant.

INTRODUCTION

Because of the requirements for increased range and speed in flying boats, an investigation of the aerodynamic characteristics of flying-boat hulls as affected by hull dimensions and hull shape is being conducted at the Langley Memorial Aeronautical Laboratory. The results of several phases of this investigation are given in references 1 to 3, which present data up to a Mach number of 0.4. The contemplated design of high-speed seaplanes has resulted in an extension of the investigation to high subsonic Mach numbers.

The present investigation was made to determine the high-speed characteristics of a flying-boat hull with high length-beam ratio, the lines of which were derived from considerations of the data given in references 1 and 2. Additional tests were made with the hull step faired and bottom rounded. For comparing the drag and stability, an investigation was also made of a streamline body simulating the fuselage of a modern transport airplane. Throughout the present paper, the hull and fuselage characteristics were derived by subtraction of wing-alone data from wing-plus-hull or -fuselage data.

COEFFICIENTS AND SYMBOLS

The results of the tests are presented as standard NACA coefficients of forces and moments. Rolling-, yawing-, and pitching-moment coefficients are given about the location (30-percent wing root chord) shown in figures 1 and 2.

In order to afford direct comparison with low-speed data the wing area, mean aerodynamic chord, and span, used in determining the coefficients and Reynolds numbers, are based on the hypothetical flying boat given in reference 1. Although these values may vary considerably from those of high-speed flying boats, it is believed that their use is justified for comparative purposes.

The hull and fuselage coefficients were derived by subtraction of wing-alone data from wing-plus-hull or -fuselage data. The wing-alone data were determined by including in the tests that part of the wing which is enclosed in the hull. The hull or fuselage coefficients therefore include the wing interference resulting from the interaction of the velocity fields of the wing and hull and also the negative wing interference caused by shielding from the air stream that part of the wing enclosed within the hull or fuselage.

The data are referred to the stability axes, which are a system of axes having their origin at the center of moments shown in figures 1 and 2 and in which the Z-axis is in the plane of symmetry and perpendicular to the relative wind, the X-axis is in the plane of symmetry and perpendicular to the Z-axis, and the Y-axis is perpendicular to the plane of symmetry. The positive directions of the stability axes are shown in figure 3.

The coefficients and symbols are defined as follows:

C_L lift coefficient $\left(\frac{\text{Lift}}{qS} \right)$

C_D drag coefficient $\left(\frac{\text{Drag}}{qS} \right)$

C_Y lateral-force coefficient $\left(\frac{Y}{qS}\right)$

C_L rolling-moment coefficient $\left(\frac{L}{qSb}\right)$

C_m pitching-moment coefficient $\left(\frac{M}{qS\bar{c}}\right)$

C_n yawing-moment coefficient $\left(\frac{N}{qSb}\right)$

Lift = $-Z$

Drag = $-X$ when $\psi = 0$

X force along X-axis, pounds

Y force along Y-axis, pounds

Z force along Z-axis, pounds

L rolling moment, foot-pounds

M pitching moment, foot-pounds

N yawing moment, foot-pounds

q free-stream dynamic pressure, pounds per square foot $\left(\frac{\rho v^2}{2}\right)$

S wing area of $\frac{1}{40.6}$ -scale model of hypothetical flying boat
(1.110 sq ft)

\bar{c} wing mean aerodynamic chord (M.A.C.) of $\frac{1}{40.6}$ -scale model of a
hypothetical flying boat (0.340 ft)

b wing span of $\frac{1}{40.6}$ -scale model of hypothetical flying boat
(3.445 ft)

V airspeed, feet per second

ρ mass density of air, slugs per cubic foot

α angle of attack of hull base line or fuselage center line, degrees

- ψ angle of yaw, degrees
- R Reynolds number, based on wing mean aerodynamic chord of hypothetical wing of $\frac{1}{40.6}$ -scale model of hypothetical flying boat
- M Mach number $\left(\frac{\text{Airspeed}}{\text{Speed of sound in air}} \right)$
- C_{m_α} rate of change of pitching-moment coefficient with angle of attack $\left(\frac{\partial C_m}{\partial \alpha} \right)$
- C_{n_ψ} rate of change of yawing-moment coefficient with angle of yaw $\left(\frac{\partial C_n}{\partial \psi} \right)$
- C_{Y_ψ} rate of change of lateral-force coefficient with angle of yaw $\left(\frac{\partial C_Y}{\partial \psi} \right)$

MODEL AND APPARATUS

The hull model had the same lines as hull 214, which had a length-beam ratio 12 (reference 1), except that the sternpost was extended to the aft perpendicular, resulting in an over-all length-beam ratio of 15, and the bow chines were rounded 7 percent of the hull length. Dimensions of the hull model are presented in figure 1 and offsets, in table I.

The general proportions of the step fairing which extended for a distance equal to nine times the depth of step at the keel are shown in figure 4. The fairing was similar to that in reference 1. For one of the tests the hull bottom was rounded over the entire length of the hull as shown in figure 5.

The streamline body which had a fineness ratio of 9.0 represents the fuselage of a typical high-speed landplane. Dimensions of the fuselage are given in figure 2 and table II.

The hull was constructed of bismuth and tin alloy built around an aluminum reinforcement beam. The step fairing and rounded bottom which was interchanged with the conventional hull bottom were of mahogany. The fuselage was aluminum. The models were attached to a steel support wing which was mounted horizontally in the tunnel on stings as shown in figure 6. The support wing which was not a scale model of the hypothetical wing used in determining the coefficients had 40° of sweepback and an NACA 63-010 airfoil section perpendicular to wing leading edge.

The support wing was set at an incidence of 0° with respect to the hull base line and fuselage center line because of structural considerations. The wing was located vertically so that the average angle of the intersections of upper and lower wing surface with the hull in the YZ-plane was the same as the average wing intersection angle on the fuselage. It is believed that this procedure reduces to a minimum the difference between that part of the wing interference drag on the hull and fuselage caused by adjoining surfaces.

The longitudinal position of the wing was determined from considerations of step location with respect to position of center of gravity on flying boats.

The volumes, surface areas, and maximum cross-sectional areas of the hull with the various refinements and of the streamline fuselage are given in table III.

TESTS

Test Conditions

The tests were made in the Langley high-speed 7- by 10-foot tunnel through the Mach number range from 0.4 to 0.85. The variation of test Reynolds number with Mach number for average test conditions is presented in figure 7. The Reynolds number was based on the mean aerodynamic chord of the hypothetical wing (0.340 ft) and was computed using a turbulence factor of unity. The degree of turbulence of the tunnel is not known but is believed to be small because of the high contraction ratio of the tunnel.

Corrections

The hull and fuselage drag coefficients have been corrected for buoyancy effects produced by the small longitudinal static-pressure gradient in the tunnel. Blocking corrections have been applied to all coefficients and Mach numbers. Angles of attack and moment data have been corrected for structural deflections caused by aerodynamic forces.

Test Procedure

The aerodynamic characteristics of the hull and fuselage with the interference of the swept support wing were determined by testing the wing alone and the wing and hull or wing and fuselage combination under approximately similar conditions. The hull or fuselage aerodynamic coefficients were then determined by subtraction, at given Mach numbers and

angles of attack, of wing-alone coefficients from the coefficients of the complete configuration after the data were cross-plotted in order to compensate for differences in Mach number and angle of attack resulting from structural deflections.

The surfaces of the hull, fuselage, and wing were smooth, and therefore transition was free, for all but one test.

RESULTS AND DISCUSSION

The data of figure 8 are typical of the final cross plots from which hull- or fuselage-plus-wing interference data were obtained. The support wing-alone drag coefficient remained constant for the range of Mach numbers tested.

The variations with Mach number of the hull and fuselage aerodynamic characteristics at angles of attack ranging from -2.0° to 7.25° are presented in figure 9; the variations with angle of attack at Mach numbers of 0.40 and 0.65 are shown in figure 10. Figure 11 presents hull and fuselage lateral aerodynamic characteristics at 0° and 4° angles of yaw. As shown in figure 10, the angles of attack for minimum drag in the positive range extended from 0° to about 4° for the hull and 0° to about 2° for the streamline body at Mach numbers for which data were not limited to low angles of attack because of structural limitations of the support wing. The angle-of-attack range for minimum drag for a comparative hull of reference 1 was from 3° to 5° . The difference is attributed mainly to the different wing incidence, 0° in the present paper and 4° in reference 1. A rapid increase in drag occurred after about 6° at Mach number of 0.4.

Transition was free for wing and fuselage for all but one test. A comparison (fig. 9(b)) of hull drag coefficient at 0° angle of attack with that of a test run where hull transition was fixed artificially by a strip of carborundum particles $\frac{1}{2}$ inch wide located approximately 5 percent of the hull length aft of the bow showed very little or no difference throughout the Mach number range tested.

Increasing Mach number resulted in drag coefficient increases for both hull and fuselage at all angles of attack investigated. However, as shown in figure 9(b), the rate of increase with Mach number became smaller as the body was made more refined. The drag coefficients at $\alpha = 0^\circ$ were 0.0023, 0.0021, 0.0017, and 0.0008 larger at 0.8 Mach number than at 0.4 Mach number for the hull, hull plus step fairing, hull with rounded bottom, and streamline body, respectively. These data indicate that a flying-boat hull of the type tested can be flown to a Mach number of 0.825 without any sharp drag rise resulting from critical shock conditions. However, because the geometric discontinuities and

flotation requirements that handicap the flying-boat hull with regard to aerodynamic performance at low speeds penalize it even more severely at high subsonic speeds, it is especially important that high-speed seaplanes incorporate new types of hulls or conventional hulls with a maximum of aerodynamic refinement.

At Mach numbers of approximately 0.4 the hull minimum drag coefficients agreed closely with that of hull model 214 given in reference 1; the hull minimum drag coefficient as given in the reference was 0.0059, whereas 0.0060 was obtained for the hull in the present investigation. The difference in Reynolds number, 3.4×10^6 for the data of reference 1 and 0.9×10^6 for the present investigation, could account for the slight increase in drag coefficient according to data presented in reference 1. The close agreement between the two values indicates that the differences in support wing and hull geometry (bow-chine fairing, sternpost location, and wing location) tended to compensate each other with regard to hull drag coefficient. This might be expected; the difference in sternpost location had little or no effect while a decrease in drag resulting from faired bow chines (reference 2) and a better wing location (reference 4) are offset by an increase in drag coefficient caused by the use of a 10-percent-chord-thick support wing instead of the 21-percent-thick wing of reference 1. The difference in hull drag coefficient resulting from different support wings should always be noted when comparisons are made with other hull-plus-wing interference data or hull-alone data. Subtraction of wing-alone data from wing-plus-hull data, as described under "Test Procedure," results in a lower drag coefficient than for hull tested alone because of the negative interference drag corresponding to that part of the wing enclosed by the hull and shielded from the air stream. If this favorable interference effect is not kept in mind when comparing with other data, the drag coefficients obtained by this method may seem abnormally low. (See reference 4.)

As in references 1 and 2, at angles of attack for minimum drag, fairing the step for a distance nine times the depth of step at the keel, as shown in figure 4, resulted in about a 0.0008 reduction in drag coefficient at about $M = 0.4$. Rounding the hull bottom completely to the shape shown in figure 5, gave a 0.0020 minimum drag coefficient reduction at 0° angle of attack; a similar alteration in reference 2 gave a reduction of 0.0019.

The minimum drag coefficient for the streamline body was 0.0030 at a Mach number of 0.4. The value obtained in reference 2 for a similar body was 0.0040. The smaller value can probably be attributed to a more favorable location of the support wing. The support wing of reference 2 protruded considerably out of the top of the fuselage; whereas the present support wing was located more towards the center of the body (fig. 2). The present wing, although thinner, has therefore a larger part shielded from the air stream which results in a large negative wing-interference

effect. Reference 4 also indicates that the present wing location produced a lower interference drag resulting from wing-fuselage juncture.

Allowing for the difference in center-of-moment position, the longitudinal stability as given by $C_{m\alpha}$ compared favorably with the values given in reference 1 for the hull and in reference 2 for the fuselage. The values of $C_{m\alpha}$ were 0.0036 and 0.0033 at 0.4 Mach number for the hull and fuselage, respectively. Increasing Mach number to 0.65 increased the value of $C_{m\alpha}$ to 0.0042 for the hull and 0.0036 for the fuselage. These changes are small, however, and correspond to an aerodynamic center shift of about 1-percent mean aerodynamic chord forward on a flying boat.

The directional stability at low Mach numbers (fig. 11) as determined by $C_{n\psi}$ was similar to that of previous tests on the hull and fuselage, as given in references 1 and 2, respectively. The value of $C_{n\psi}$ was 0.0010 for the hull and 0.0005 for the fuselage. Increasing Mach number increased the directional instability slightly for the hull; that is, the value of $C_{n\psi}$ was increased to 0.0012. Increasing Mach number had only a slight effect on the directional instability for the fuselage.

The value of $C_{Y\psi}$ was 0.006 for the hull and 0.001 for the fuselage; these values were in good agreement with previous tests at low Mach numbers and had little or no variation with Mach number.

For convenience the stability parameters and minimum drag coefficients are listed in table IV.

CONCLUSIONS

The results of tests in the Langley 7- by 10-foot high-speed tunnel to determine the effect of Mach number on the aerodynamic characteristics of a flying-boat hull with high length-beam ratio and testing of a streamline body for comparison with the flying-boat hull indicate the following conclusions:

1. Increasing Mach number resulted in drag coefficient increases for both hull and fuselage at all angles of attack investigated; the rate of increase became smaller as the body was made more refined. At 0° angle of attack the drag coefficients were 0.0023, 0.0021, 0.0017, and 0.0008 larger at 0.8 Mach number than at 0.4 Mach number for the hull, hull with step fairing, hull with rounded bottom, and streamline body, respectively.

2. Angles of attack for minimum drag in the positive range extended from 0° to about 4° for the hull and 0° to about 2° for the streamline

body for all Mach numbers at which data were not limited to low angles of attack.

3. Increasing Mach number resulted in a very slight decrease in longitudinal stability for both hull and fuselage; directional stability was generally constant.

Langley Memorial Aeronautical Laboratory
National Advisory Committee for Aeronautics
Langley Field, Va.

REFERENCES

1. Yates, Campbell C., and Riebe, John M.: Effect of Length-Beam Ratio on the Aerodynamic Characteristics of Flying-Boat Hulls. NACA TN No. 1305, 1947.
2. Riebe, John M., and Naeseth, Rodger L.: Effect of Aerodynamic Refinement on the Aerodynamic Characteristics of a Flying-Boat Hull. NACA TN No. 1307, 1947.
3. Yates, Campbell C., and Riebe, John M.: Aerodynamic Characteristics of Three Planing-Tail Flying-Boat Hulls. NACA TN No. 1306, 1947.
4. Jacobs, Eastman N., and Ward, Kenneth E.: Interference of Wing and Fuselage from Tests of 209 Combinations in the N.A.C.A. Variable-Density Tunnel. NACA Rep. No. 540, 1935.

TABLE I.- OFFSETS FOR LANGLEY TANK MODEL 214 MODIFIED WITH EXTENDED AFTERBODY AND ROUNDED BOW CHINES

[All dimensions are in inches]

Station	Distance to F.P.	Keel above \bar{x}	Chine above \bar{x}	Half beam at chine	Radius and half maximum beam	Height of hull at \bar{x}	Line of centers above \bar{x}	Angle of chine flare (deg)	Forebody bottom, heights above \bar{x}									
									Butt 0.10	Butt 0.20	Butt 0.31	Butt 0.41	Butt 0.51	Butt 0.61	Butt 0.71	Butt 0.81	Butt 0.92	
F.P.	0	2.50	-----	-----	0	2.74	-----	-----										
1/2	.58	1.35	-----	-----	.47	3.52	3.05	-----	1.55	1.76	1.89	1.93						
1	1.15	.93	-----	-----	.62	3.87	3.25	-----	1.08	1.24	1.40	1.50	1.54	1.53				
2	2.30	.45	1.01	0.79	.79	4.28	3.49	10	.57	.68	.80	.89	.97	1.01	1.02			
3	3.46	.20	.69	.88	.88	4.54	3.66	10	.28	.37	.45	.54	.61	.67	.69	0.70		
4	4.61	.07	.49	.94	.94	4.71	3.77	10	.13	.20	.27	.33	.40	.45	.49	.51	0.50	
5	5.76	.01	.37	.98	.98	4.83	3.85	10	.06	.11	.17	.21	.27	.31	.35	.37	.38	
6	6.91	0	.31	1.00	1.00	4.90	3.90	5	.04	.08	.12	.16	.20	.24	.27	.30	.31	
7	8.07	0	.29	1.00	1.00	4.92	3.92	0	.04	.07	.11	.15	.19	.22	.25	.27	.29	
8	9.22	0	.29	1.00	1.00	4.93	3.92	0	.04	.07	.11	.15	.19	.22	.25	.27	.29	
9	10.37	0	.29	1.00	1.00	4.93	3.92	0	.04	.07	.11	.15	.19	.22	.25	.27	.29	
10	11.52	0	.29	1.00	1.00	4.93	3.92	0	.04	.07	.11	.15	.19	.22	.25	.27	.29	
11	12.67	0	.29	1.00	1.00	4.93	3.92	0	.04	.07	.11	.15	.19	.22	.25	.27	.29	
12F	13.84	0	.29	1.00	1.00	4.93	3.92	0	.04	.07	.11	.15	.19	.22	.25	.27	.29	
12A	13.84	.29	.65	1.00	1.00	4.93	3.92											
13	14.98	.46	.82	1.00	1.00	4.93	3.93											
14	16.13	.63	.99	.99	.99	4.93	3.94											
15	17.28	.80	1.15	.97	.97	4.93	3.96											
16	18.43	.97	1.31	.94	.94	4.93	3.99											
17	19.58	1.14	1.46	.89	.89	4.93	4.02											
18	20.74	1.31	1.62	.84	.84	4.93	4.09											
19	21.89	1.48	1.76	.78	.78	4.93	4.15											
20	23.04	1.65	1.91	.71	.71	4.93	4.22											
21	24.19	1.82	2.05	.62	.62	4.93	4.30											
22	25.35	1.99	2.19	.53	.53	4.93	4.39											
23	26.50	2.16	2.32	.43	.43	4.93	4.50											
24	27.65	2.33	2.45	.32	.32	4.93	4.60											
25	28.80	2.50	2.58	.21	.21	4.93	4.72											
26	29.95	2.67	2.70	.08	.08	4.93	4.84											
A.P.	30.00	2.69	2.71	.08	.08	4.93	4.85											

Radius and half maximum beam

Height of hull at \bar{x}

Straight line

Angle of chine flare

Butt

chine above \bar{x}

Keel above \bar{x}

Line of centers

Half beam at chine

Forebody

Afterbody

NACA

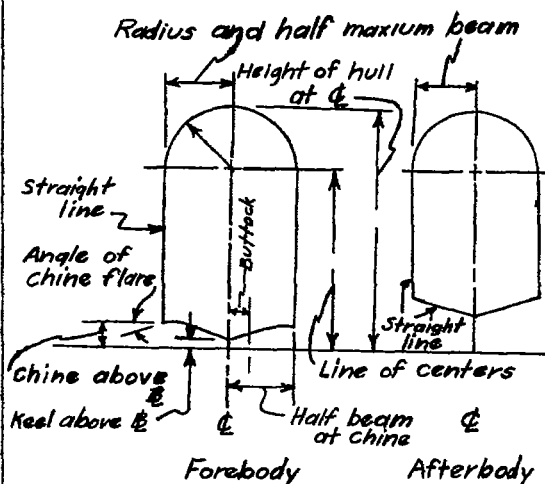


TABLE II.— ORDINATES FOR STREAMLINE BODY

[All dimensions are given in inches]

Station	Radius	Station	Radius
0	0	12.180	1.661
.041	.105	13.068	1.651
.135	.215	13.919	1.645
.270	.324	14.902	1.629
.540	.484	15.959	1.603
.865	.631	17.013	1.569
1.297	.787	17.914	1.533
2.026	.990	18.596	1.500
2.161	1.022	19.582	1.446
2.769	1.152	20.464	1.389
3.620	1.298	21.538	1.308
4.474	1.408	22.436	1.229
5.275	1.484	23.327	1.141
6.045	1.539	24.219	1.040
6.787	1.578	25.110	.927
7.564	1.608	26.002	.799
8.466	1.632	26.870	.660
9.462	1.649	27.717	.507
10.299	1.657	28.589	.331
11.204	1.661	29.352	.160
11.576	1.661	30.000	0



TABLE III.— VOLUMES, SURFACE AREAS, AND MAXIMUM CROSS-SECTIONAL AREAS
OF LANGLEY TANK MODEL 214 MODIFIED WITH EXTENDED AFTERBODY
AND FAIRED NOSE AND OF STREAMLINE FUSELAGE

Configuration	Volume (cu in.)	Surface area (sq in.)	Maximum cross- sectional area (sq in.)
Hull	177	282	9.16
Hull, step faired	178	284	9.16
Hull, bottom rounded	172	281	9.00
Streamline fuselage	172	238	8.65



TABLE IV.— DRAG COEFFICIENTS AND STABILITY PARAMETERS OF LANGLEY TANK

MODEL 214 MODIFIED WITH EXTENDED AFTERBODY AND FAIRED

NOSE AND OF STREAMLINE FUSELAGE

Configuration	$C_{D_{min}}$		$\frac{\partial C_m}{\partial \alpha}$		$\frac{\partial C_n}{\partial \psi}$ for $\alpha = 0^\circ$		$\frac{\partial C_y}{\partial \psi}$ for $\alpha = 0^\circ$	
	M = 0.40	M = 0.80	M = 0.40	M = 0.65	M = 0.40	M = 0.80	M = 0.40	M = 0.80
Hull	0.0060	0.0080	0.0036	0.0042	0.0010	0.0012	0.006	0.006
Hull, step faired	.0050	.0062	.0036	.0042				
Hull, bottom rounded	^a .0040	^a .0056						
Streamline fuselage	.0030	.0035	.0033	.0036	.0005	.0005	.001	.001

^aAt $\alpha = 0^\circ$.

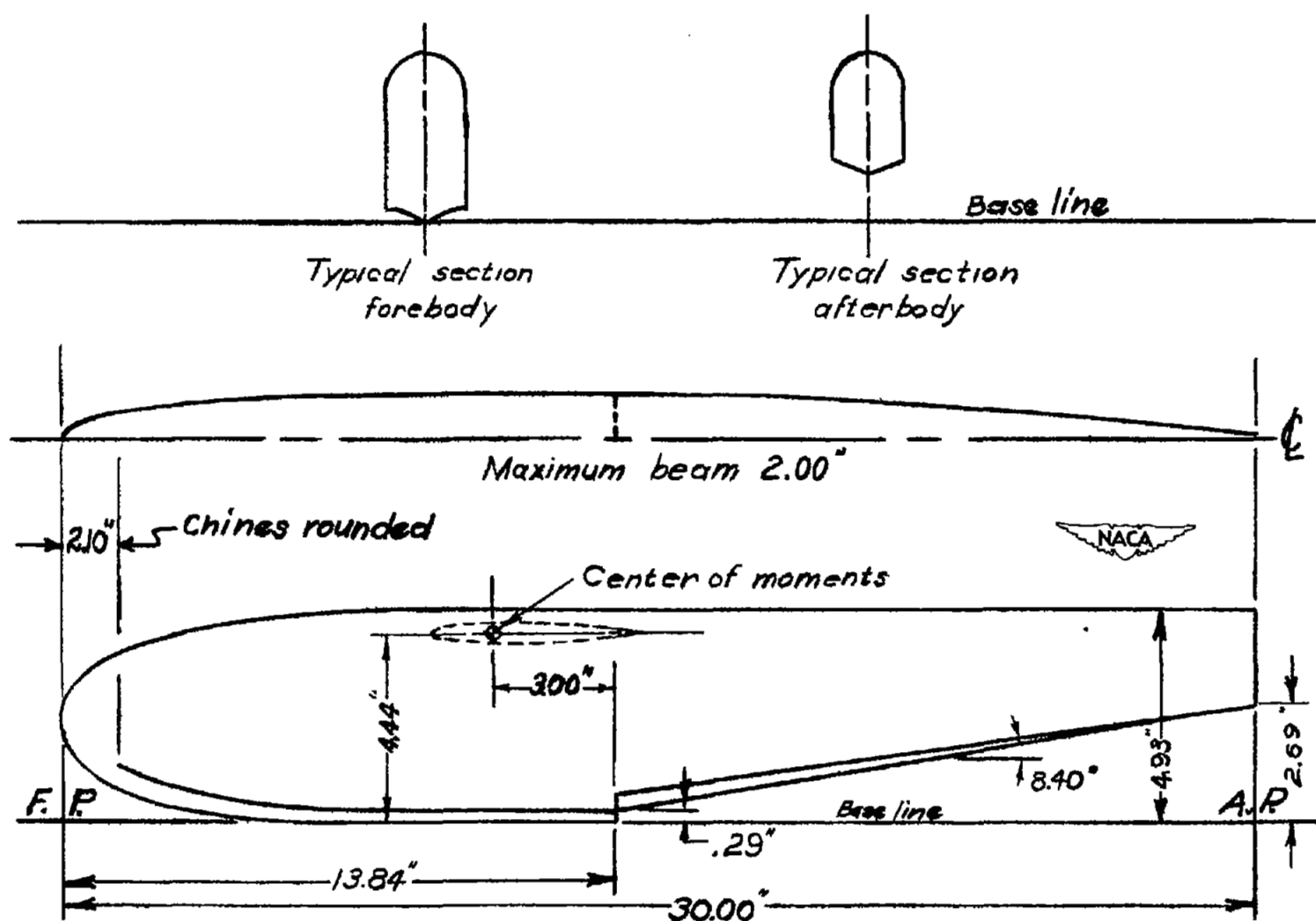



Figure 1.- Lines of Langley tank model 214 modified with extended afterbody and rounded bow chines.

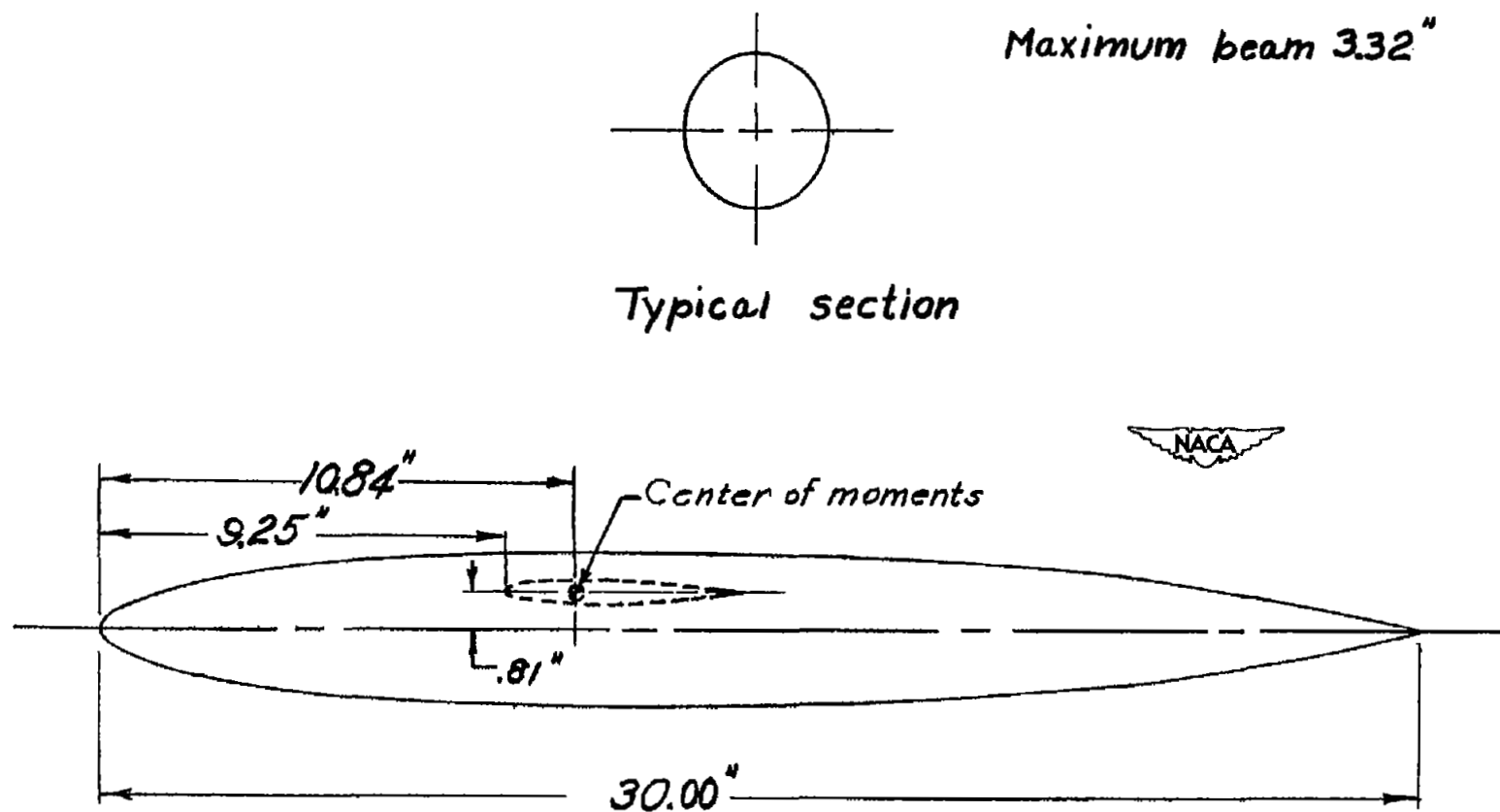


Figure 2.- Lines of streamline body.

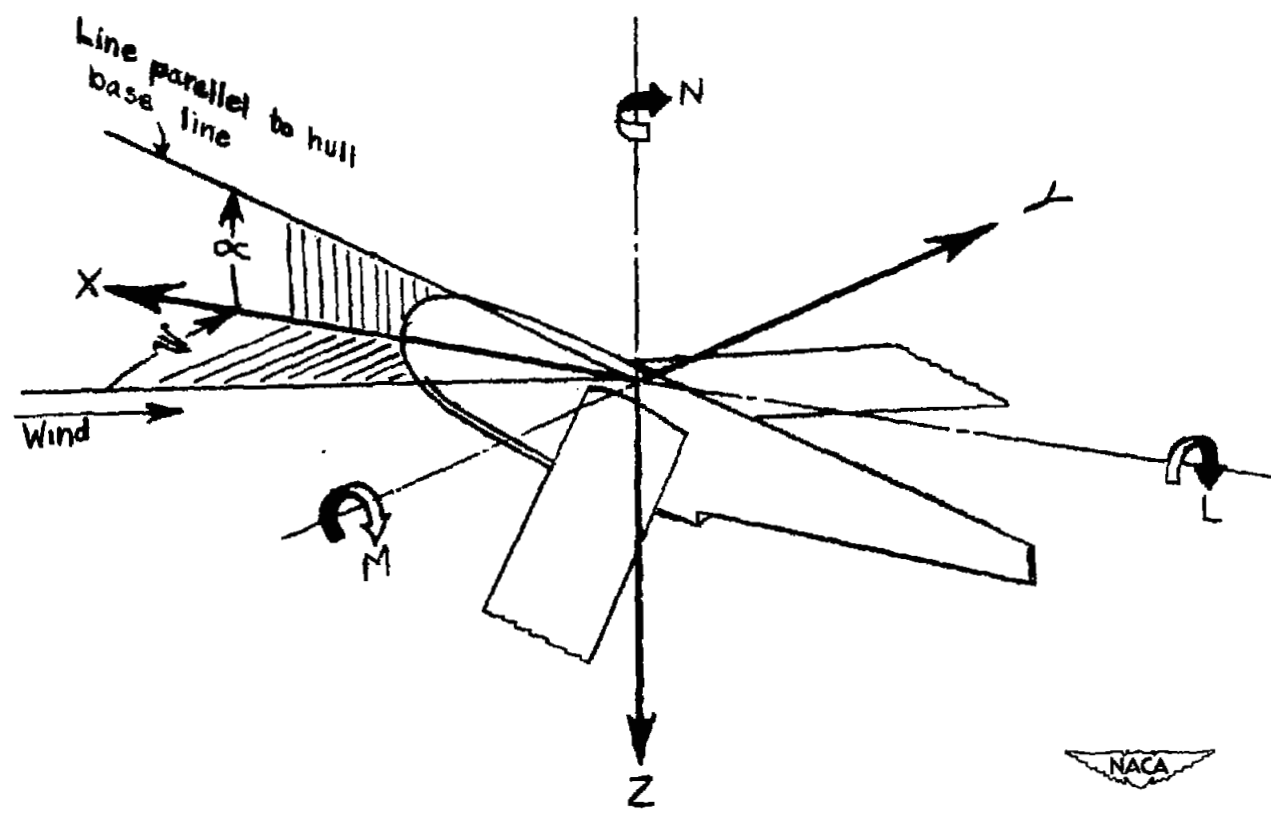


Figure 3.- System of stability axes. Positive values of forces, moments, and angles are indicated by arrows.

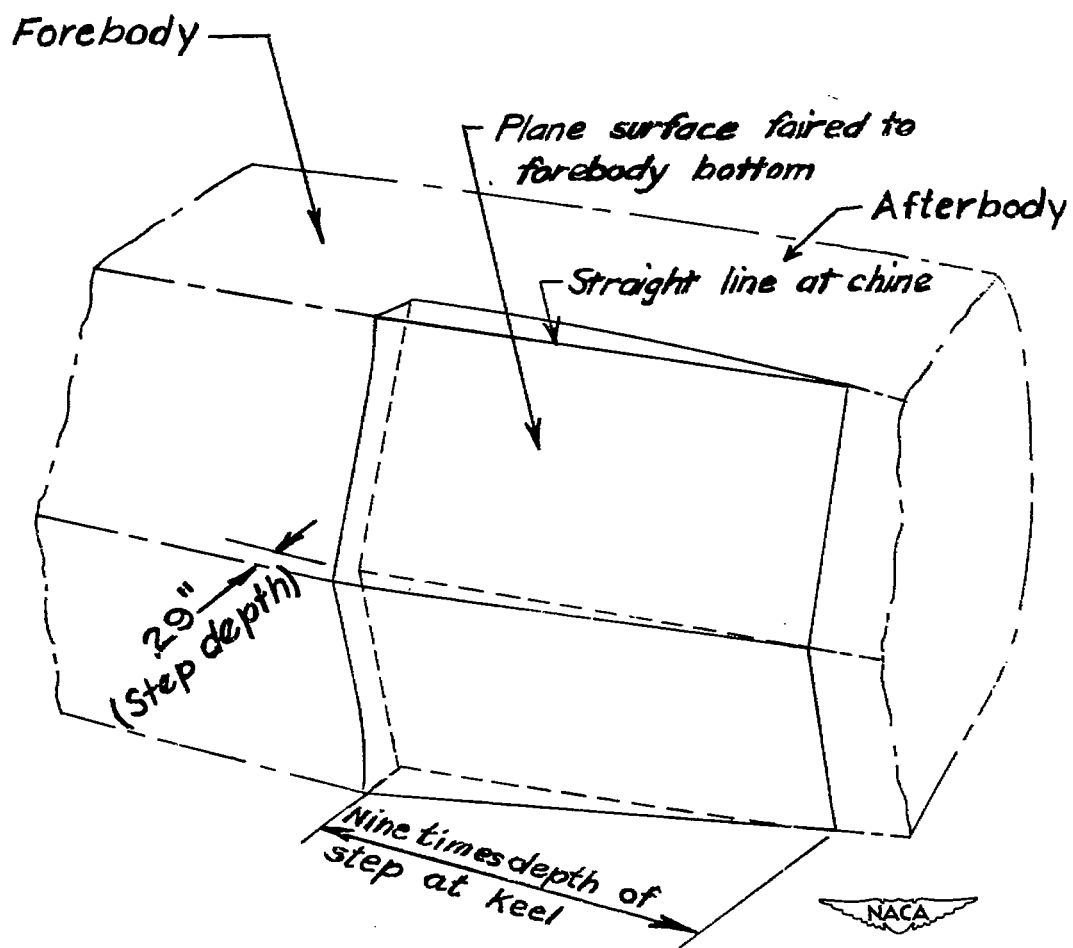


Figure A.- General details of step faired nine times depth of step at keel. Bottom view of hull.

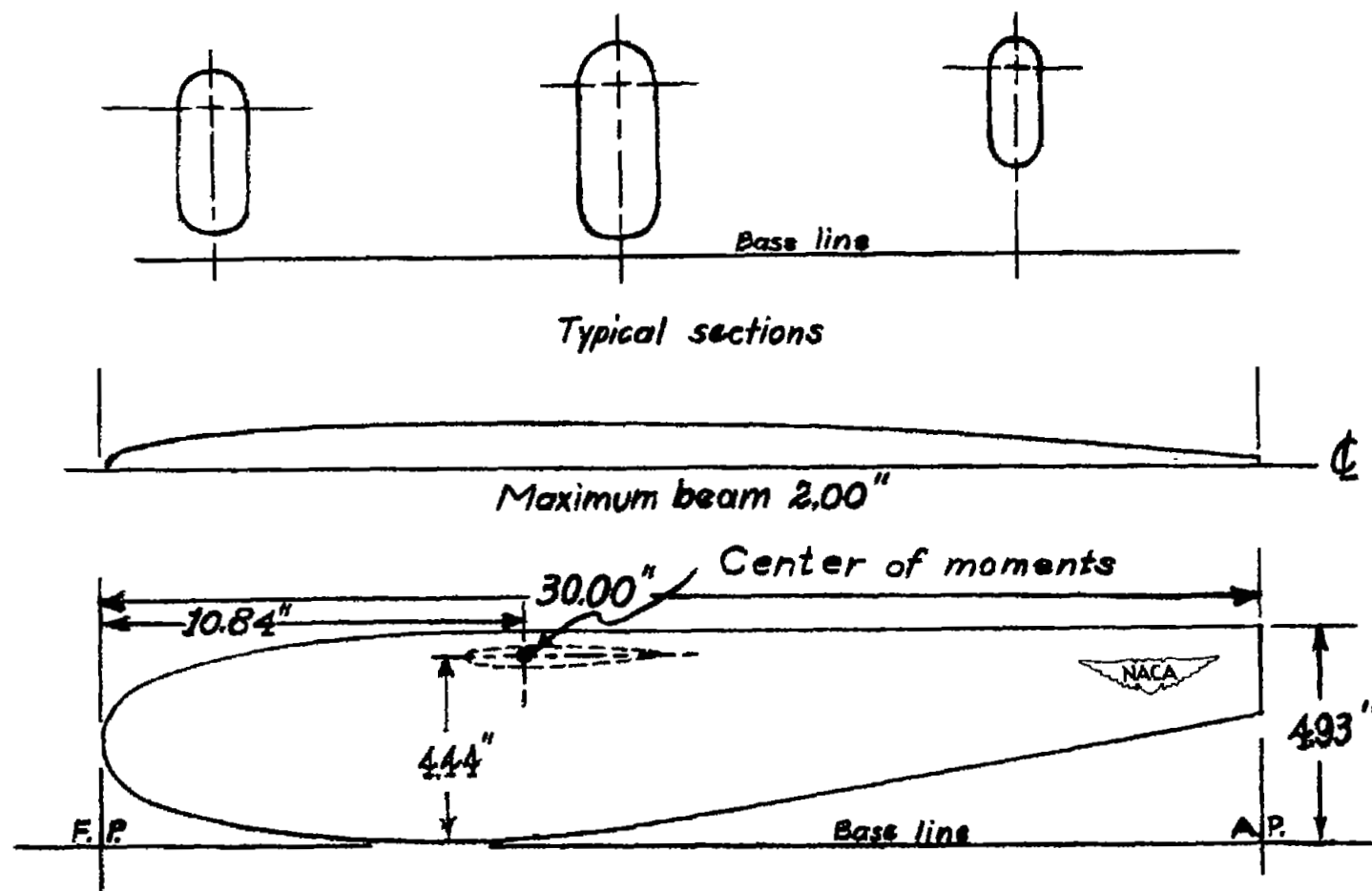


Figure 5.- Lines of Langley tank model 214 modified with rounded bottom.



Figure 6.- Langley tank model 214 modified with extended afterbody, bow chines rounded and step faired, mounted in the Langley 7- by 10-foot high-speed tunnel.

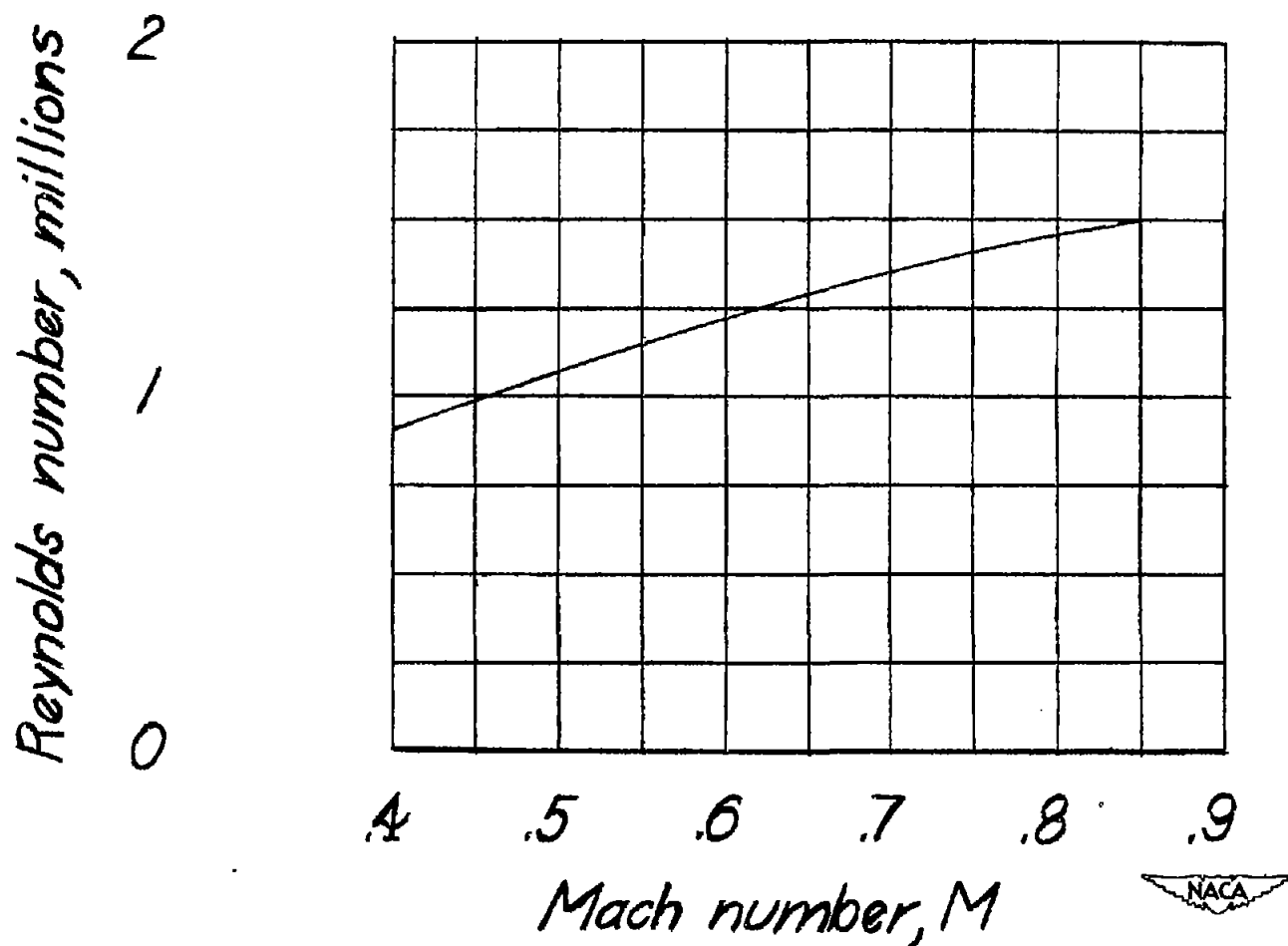


Figure 7. - Variation of test Reynolds number with Mach number for a high length-beam ratio flying-boat hull and streamline body. Reynolds number based on hypothetical wing chord.

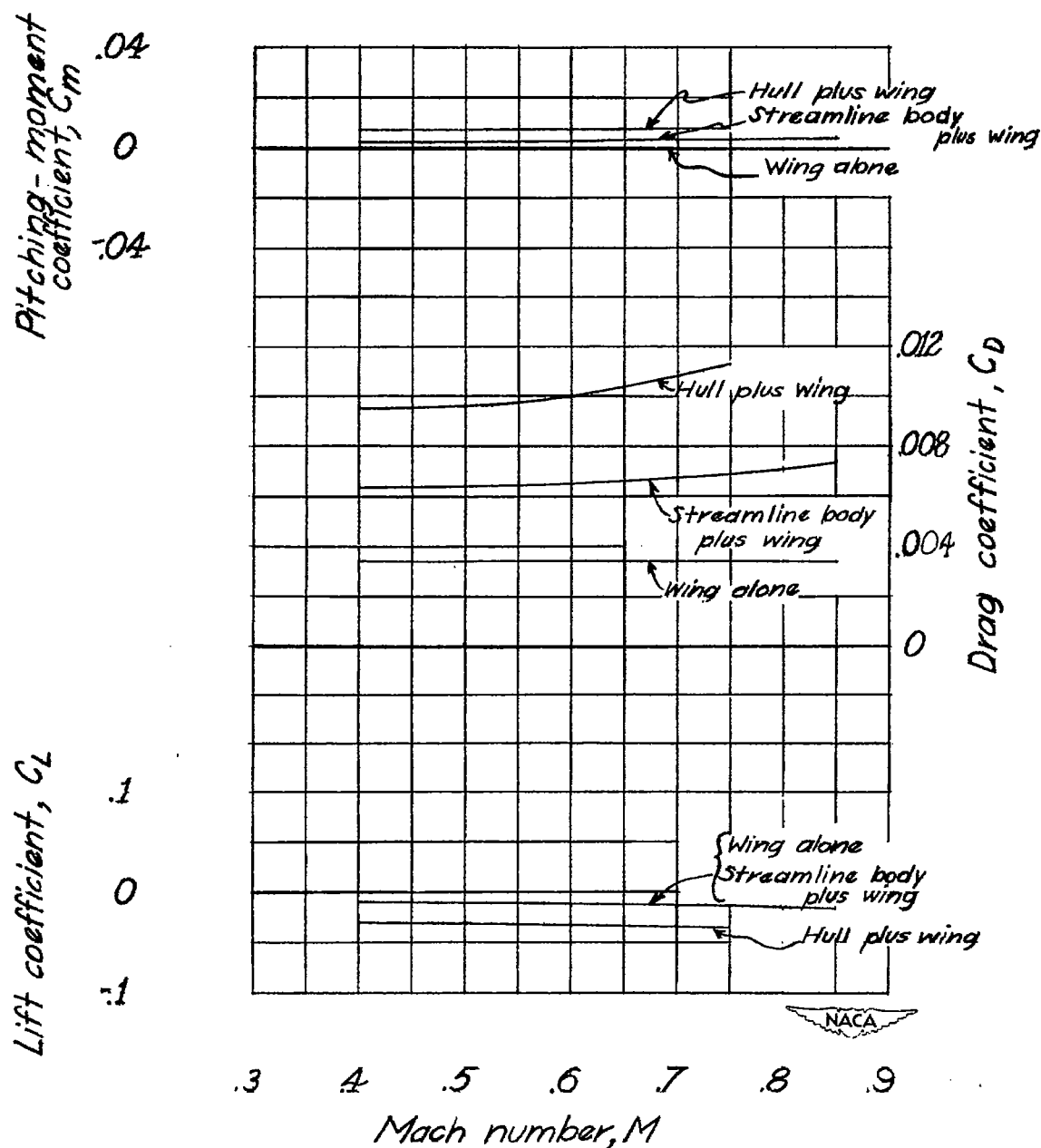


Figure 8.- Variation with Mach number of the aerodynamic characteristic of a high-length-beam-ratio flying-boat hull plus support wing, streamlined body plus support wing, and support wing alone; $\alpha=0^\circ$.

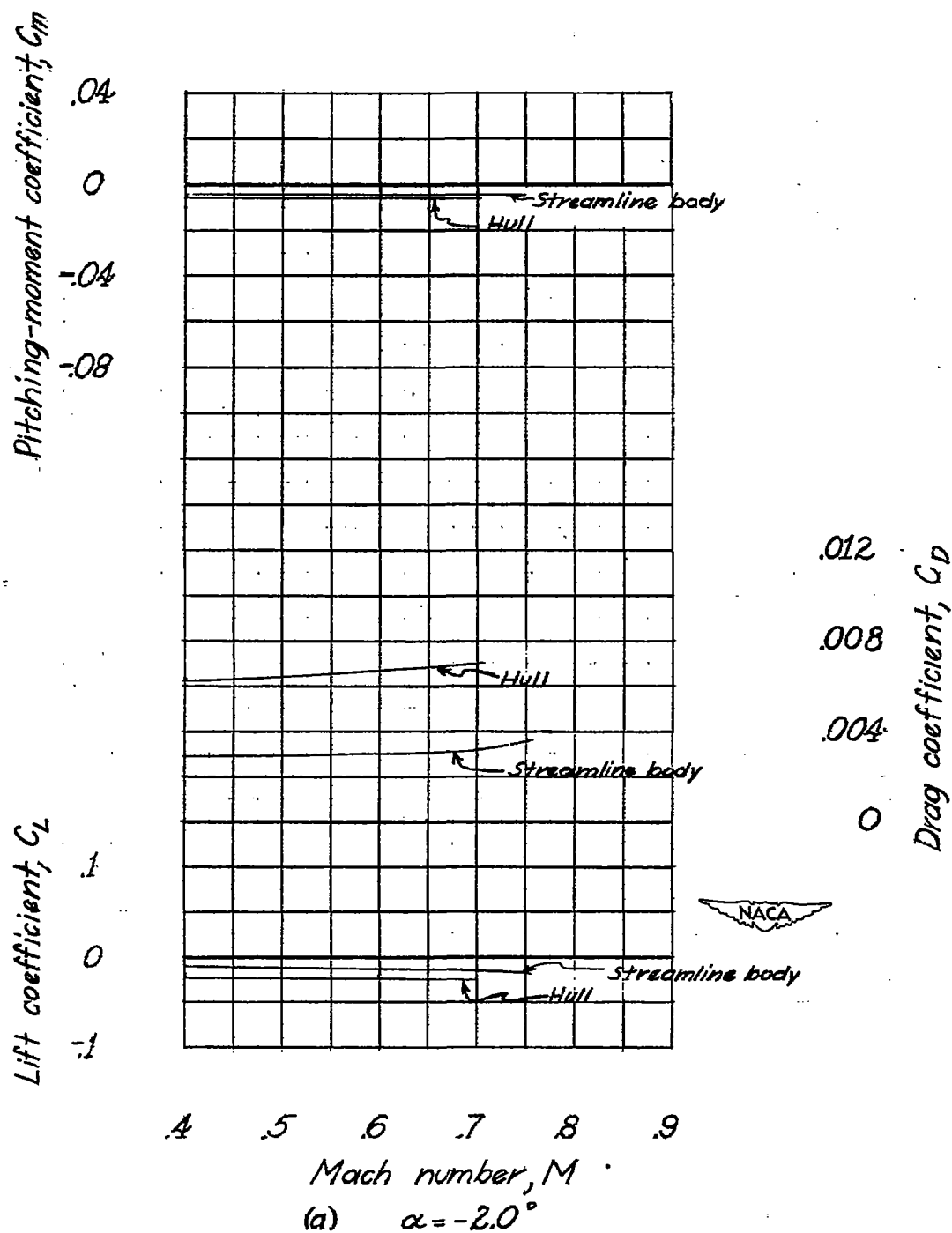


Figure 9.- Effect of Mach number on the aerodynamic characteristics of a high-length-beam-ratio flying boat hull and a streamline body.

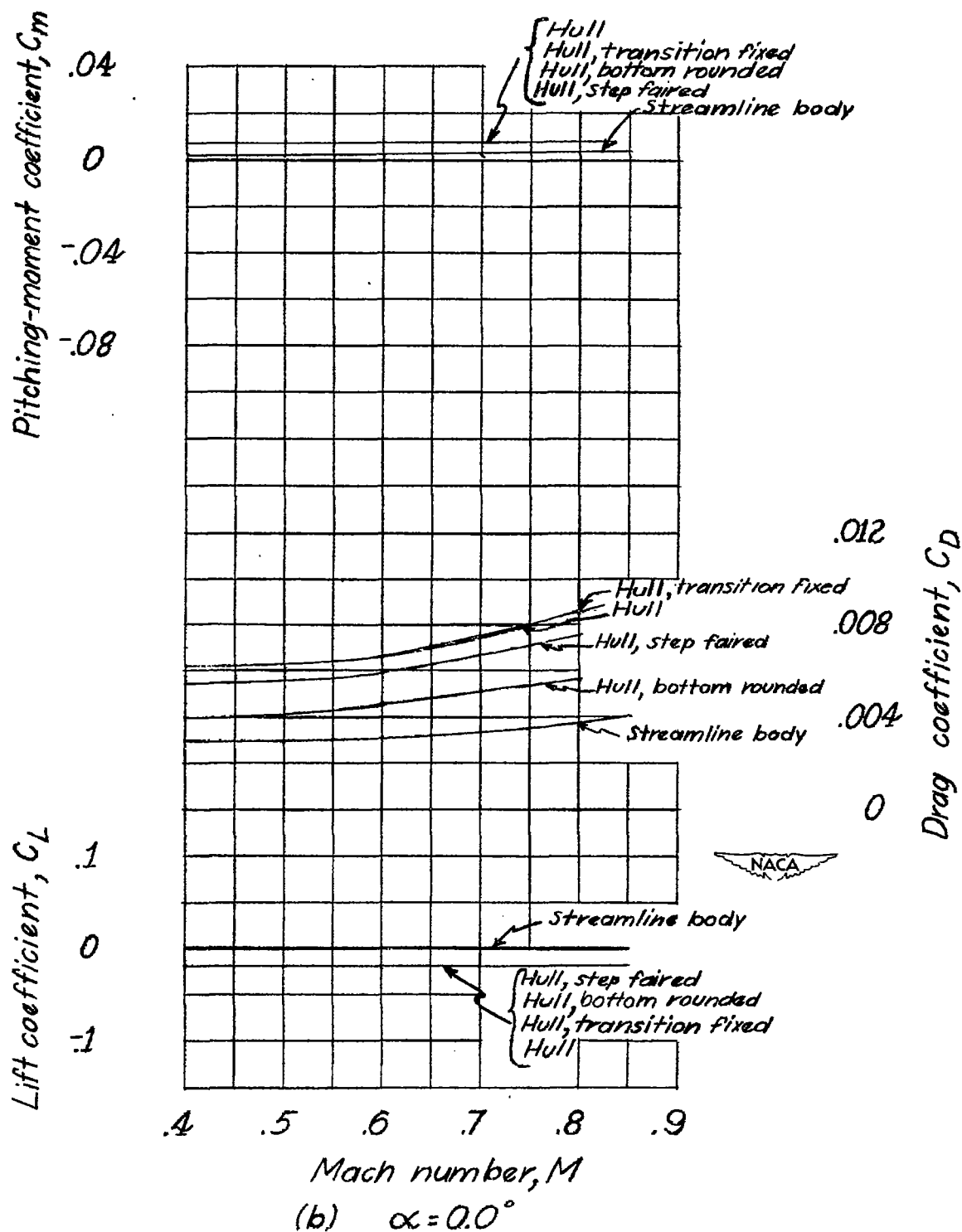


Figure 9.- Continued

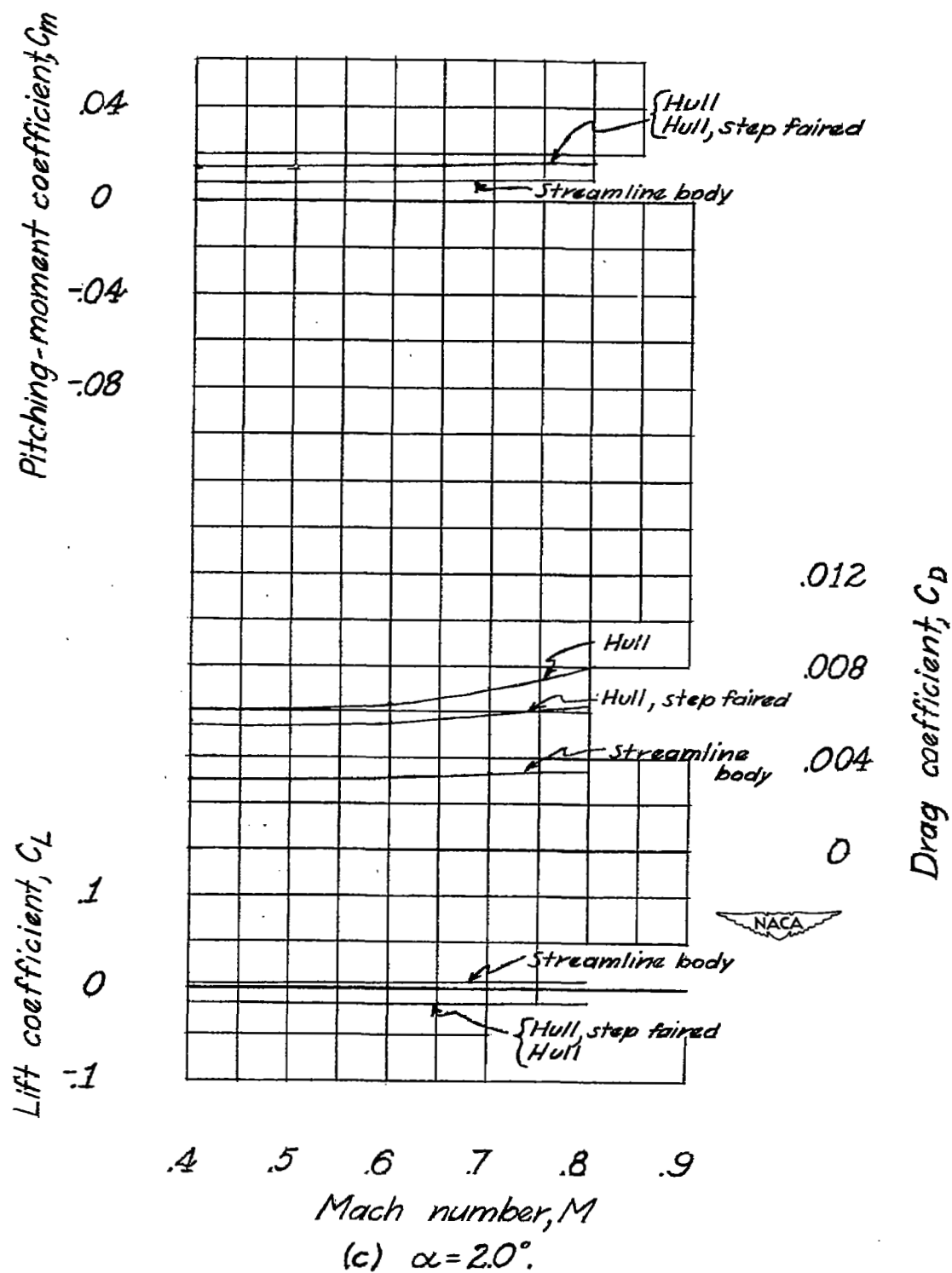


Figure 9.- Continued.

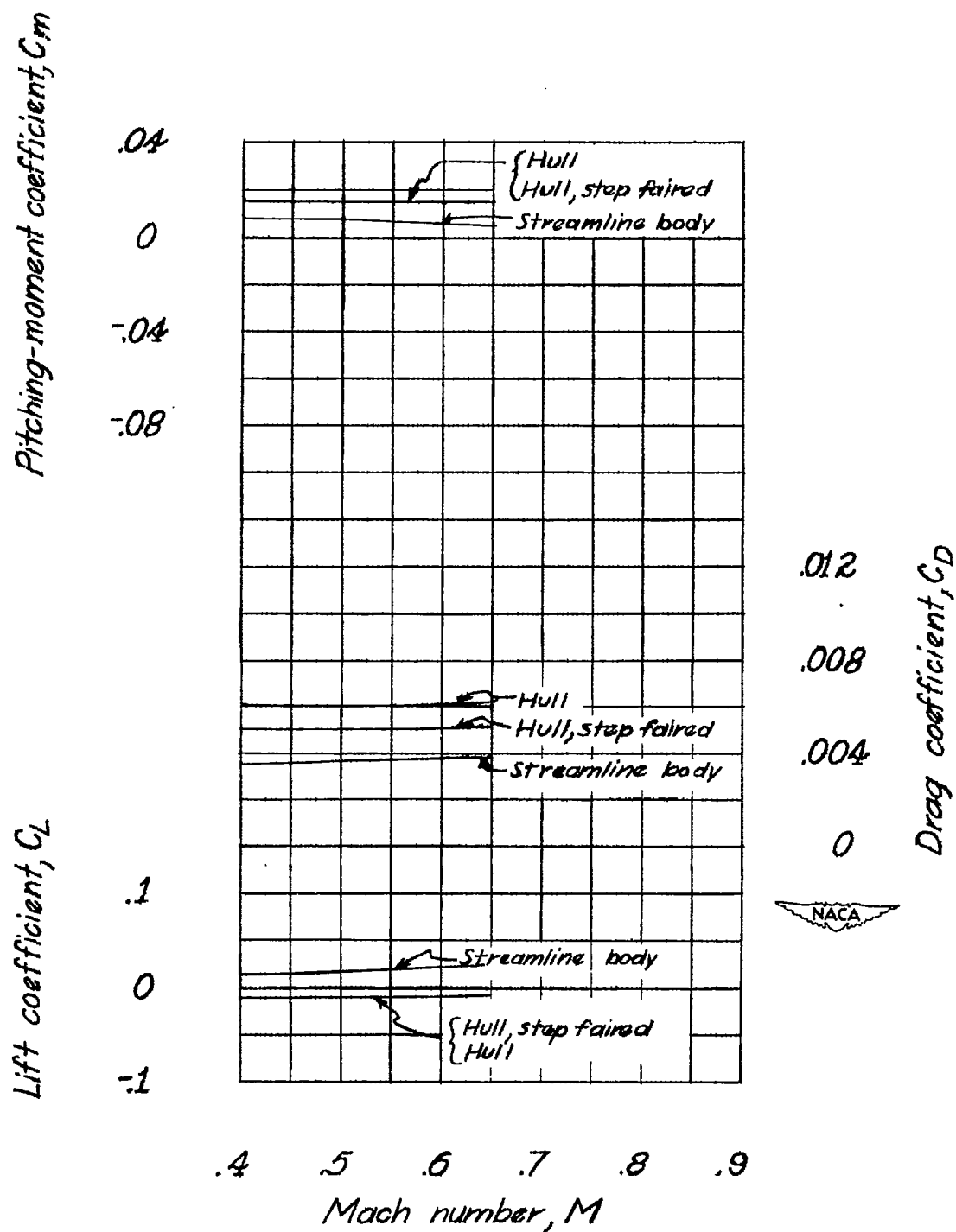


Figure 9.- Continued.

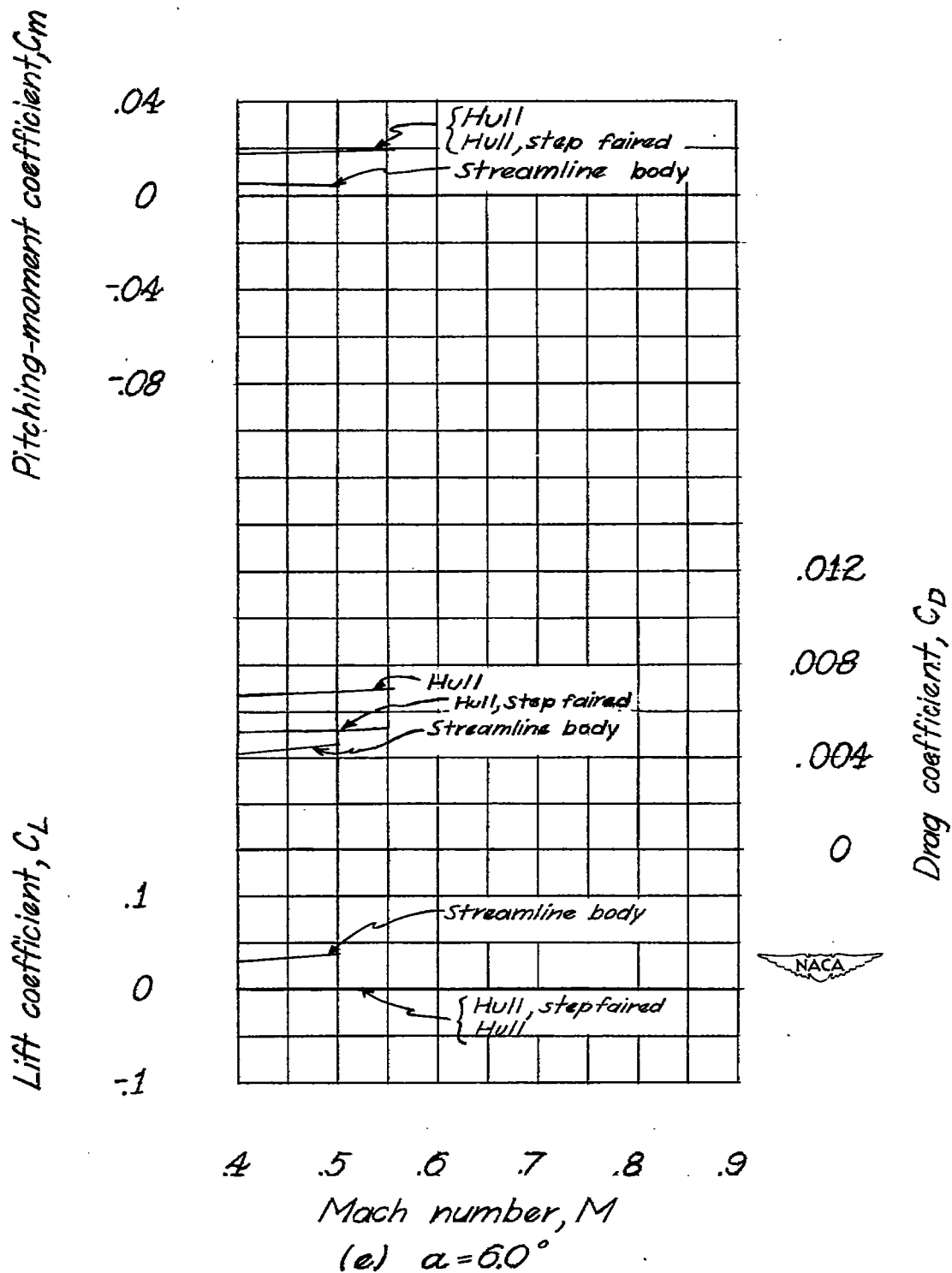


Figure 9. - Continued.

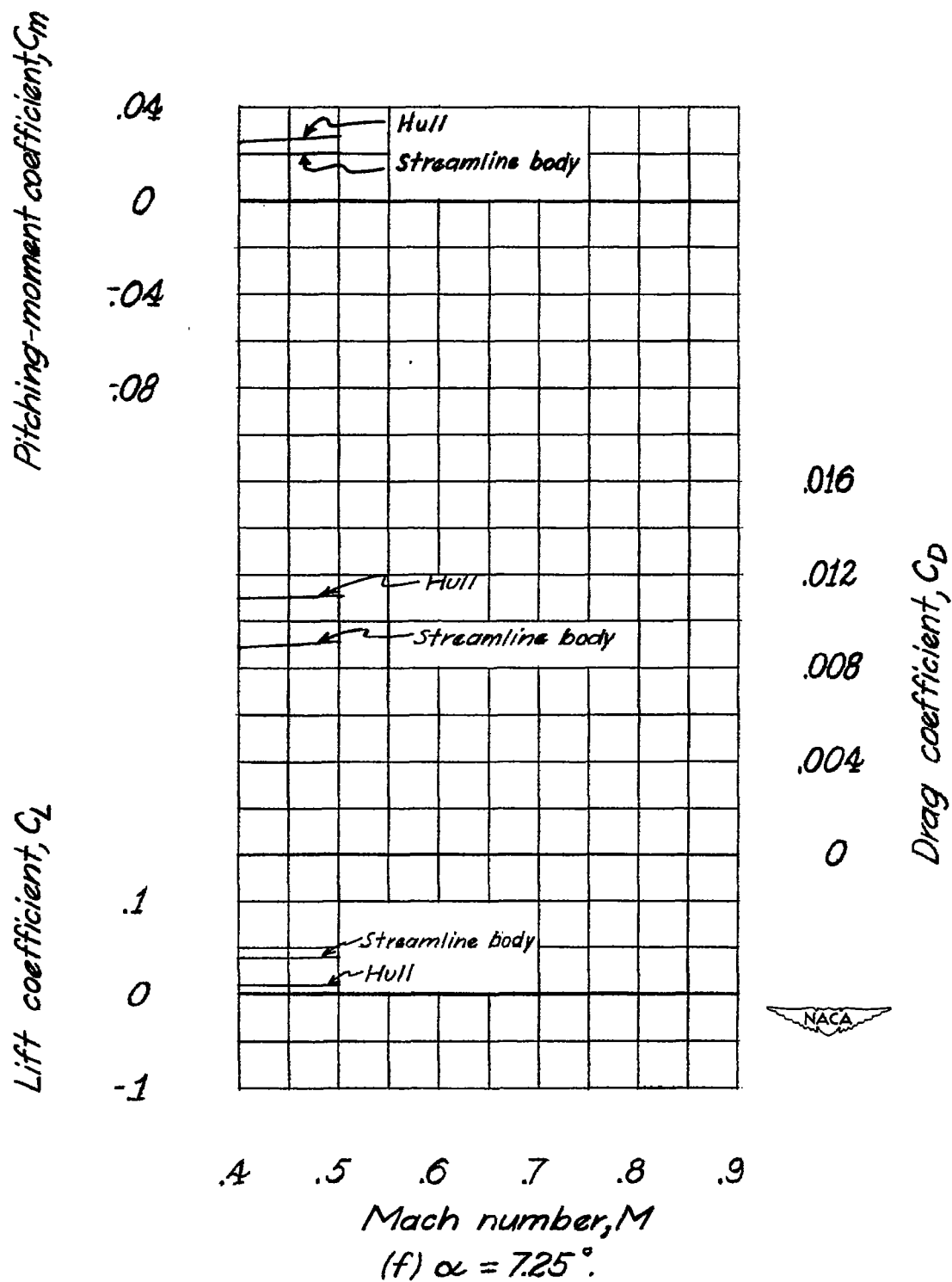


Figure 9.- Concluded.

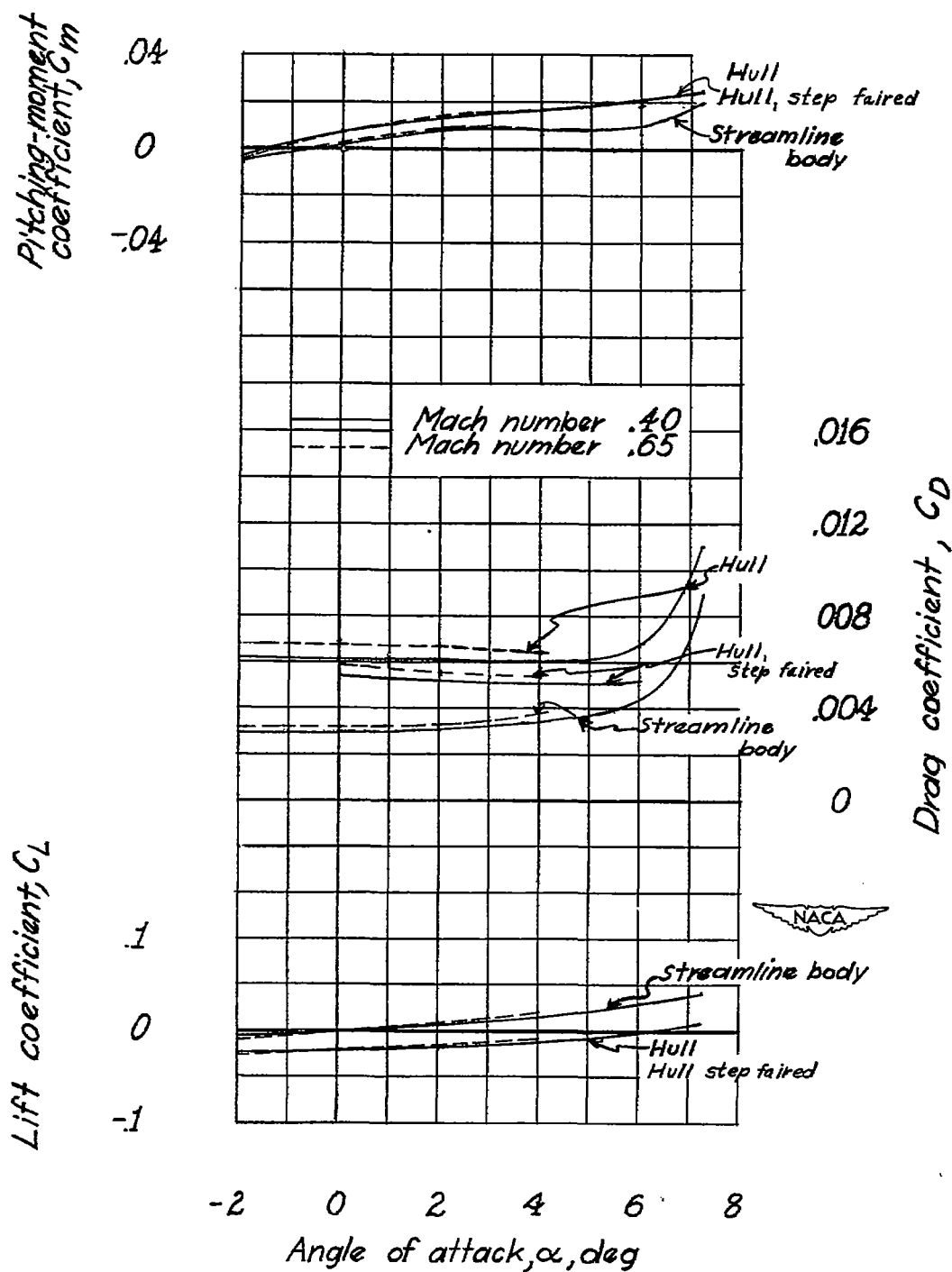


Figure 10.- The aerodynamic characteristics in pitch of a high-length-beam-ratio flying-boat hull and a streamlined body.

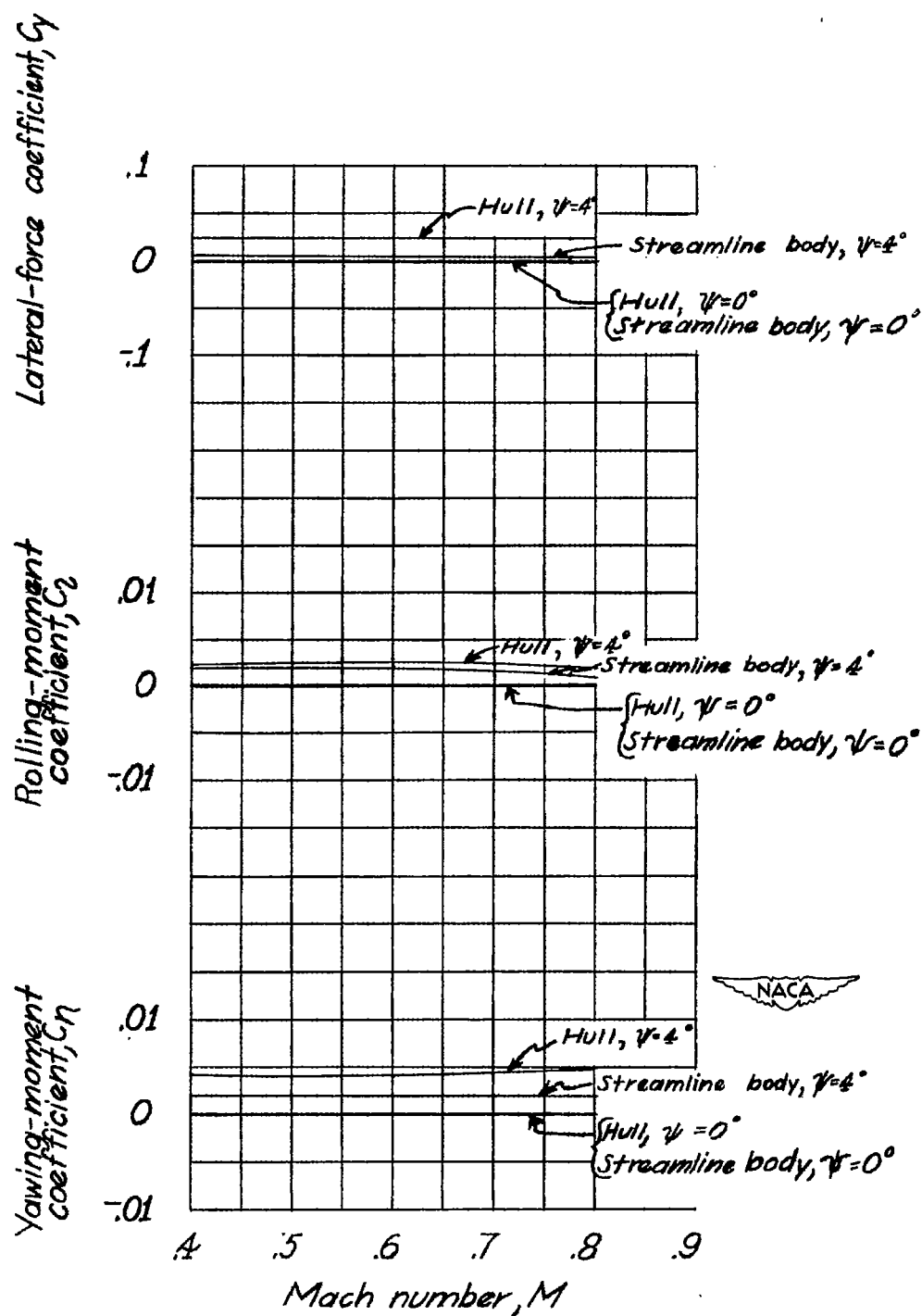
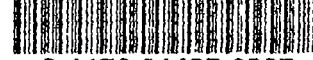


Figure 11.- Variation with Mach number of the aerodynamic characteristics in yaw of a high-length-beam-ratio hull and a streamline body; $\alpha=0^\circ$.

NASA Technical Library



3 1176 01435 9385